

# Ground-state hyperfine structure of H-, Li-, and B-like ions in middle- $Z$ region

A. V. Volotka,<sup>1,2</sup> D. A. Glazov,<sup>2</sup> I. I. Tupitsyn,<sup>2</sup> N. S. Oreshkina,<sup>2</sup> G. Plunien,<sup>1</sup> and V. M. Shabaev<sup>2</sup>

<sup>1</sup> *Institut für Theoretische Physik,*

*Technische Universität Dresden,*

*Mommsenstraße 13,*

*D-01062 Dresden, Germany*

<sup>2</sup> *Department of Physics,*

*St. Petersburg State University,*

*Oulianovskaya 1, Petrodvorets,*

*198504 St. Petersburg, Russia*

## Abstract

The hyperfine splitting of the ground state of H-, Li-, and B-like ions is investigated in details within the range of nuclear numbers  $Z = 7 - 28$ . The rigorous QED approach together with the large-scale configuration-interaction Dirac-Fock-Sturm method are employed for the evaluation of the interelectronic-interaction contributions of first and higher orders in  $1/Z$ . The screened QED corrections are evaluated to all orders in  $\alpha Z$  utilizing an effective potential approach. The influence of nuclear magnetization distribution is taken into account within the single-particle nuclear model. The specific differences between the hyperfine-structure level shifts of H- and Li-like ions, where the uncertainties associated with the nuclear structure corrections are significantly reduced, are also calculated.

PACS numbers: 32.10.Fn, 31.15.aj, 31.30.J-

## I. INTRODUCTION

Accurate knowledge of the hyperfine structure lines of middle- $Z$  multicharged ions is of great interest due to suggested observations of these lines from hot rarefied astrophysical plasmas [1, 2]. Such observations may allow one to study the chemical and isotopic compositions of the supernova remnants, and the hot interstellar medium, including the galactic halos, which are the main types of objects from which intense emission lines are expected. The experiments on the determination of hyperfine splittings will also enable us to refine the deduction of nuclear magnetic moments of different isotopes and to inspect the various computational models employed for the theoretical description of nuclear effects. High-precision measurements of the ground-state hyperfine structure of heavy highly charged ions have been performed in Refs. [3, 4, 5, 6, 7]. Extension of these experiments to Li-like ions presently being prepared [8] will provide tests of quantum electrodynamics (QED) in strong electric and magnetic fields on level of a few percent in specific difference of the hyperfine splitting values of H- and Li-like ions [9]. In this difference the main theoretical uncertainty which originates from the nuclear magnetization distribution correction (Bohr-Weisskopf effect) is essentially reduced. In specific differences of heavy H- and B-like ions or Li- and B-like ions the same reduction of the theoretical uncertainty can be also achieved. This becomes clear from the approximate analytical expressions for the Bohr-Weisskopf correction given in Ref. [10].

The theoretical investigations of the hyperfine splitting of H- and Li-like multicharged ions in the middle- $Z$  region have some history. The first accurate calculation ( $\sim 0.1\%$ ), based on a combination of  $1/Z$  perturbation theory and the nonrelativistic configuration-interaction Hartree-Fock method, was performed in Refs. [11, 12]. Later, Boucard and Indelicato [13] employing the multi-configuration Dirac-Fock method presented the evaluation of the hyperfine splitting values over the entire range of the nuclear charge numbers  $Z = 3 - 92$ . Expansion in  $\alpha Z$  of the QED correction has been worked out in Refs. [14, 15, 16] (for earlier studies see references therein and recent reviews [17, 18]). However, the application of the  $\alpha Z$ -expansion is restricted to  $s$ -states in one-electron ions and limited by its convergence property. Therefore, we evaluate the radiative corrections numerically to all orders in  $\alpha Z$  accounting for the interelectronic-interaction effects by means of local screening potentials. All-order calculations of one-loop QED contributions to the hyperfine structure for middle- $Z$  ions have been previously performed for the  $1s$  state [19, 20, 21, 22], for the  $2s$  state [21, 22], and for the  $2p_{1/2}$  state [23]. However, almost all these calculations of the QED corrections were dealing with one-electron ions only, where the screening effects are

absent.

In the present paper, we calculate the ground-state hyperfine structure of H-, Li-, and B-like sequences in the middle- $Z$  region. The one-loop radiative corrections are evaluated to all orders in  $\alpha Z$  employing an effective local screening potential. Many-body effects are taken into account to the first order in  $1/Z$  within the QED perturbation theory and to higher orders within the large-scale configuration-interaction Dirac-Fock-Sturm method (CI-DFS). The single-particle nuclear model is employed for the evaluation of the Bohr-Weisskopf correction. The main goal of this work is to improve the accuracy of previous results for the hyperfine structure of H- and Li-like ions and to present novel calculations for the B-like sequence in the middle- $Z$  region.

The paper is organized as follows: In the next section the basic formulas for the hyperfine splitting are given and the derivation of the various contributions is described. In Section III we present the numerical results for all contributions and compare the total values with previously reported calculations and with existing experimental data. Section IV provides a complete compilation of the total values for the hyperfine splitting of H-, Li, and B-like ions as well as the results for the specific differences between the hyperfine structure of H- and Li-like ions. We close with a short summary and point out the main achievements of the present work.

Relativistic units ( $\hbar = 1$ ,  $c = 1$ ,  $m = 1$ ) and the Heaviside charge unit [ $\alpha = e^2/(4\pi)$ ,  $e < 0$ ] are used throughout the paper.

## II. BASIC EXPRESSIONS

The interaction of atomic electrons with the nuclear magnetic-dipole moment is described by the Fermi-Breit operator, which is conveniently written as a scalar product of two tensor operators

$$H_\mu = \frac{|e|}{4\pi} \boldsymbol{\mu} \cdot \mathbf{T}, \quad (1)$$

where  $\boldsymbol{\mu}$  is the nuclear magnetic moment operator acting in the space of nuclear states. The electron part  $\mathbf{T}$  is defined by the following expression

$$\mathbf{T} = \sum_i \frac{[\mathbf{n}_i \times \boldsymbol{\alpha}_i]}{r_i^2}, \quad (2)$$

where index  $i$  refers to the  $i$ -th electron of the atom,  $\boldsymbol{\alpha}$  is the Dirac-matrix vector, and  $\mathbf{n}_i = \mathbf{r}_i/r_i$ . This interaction leads to the hyperfine splitting of the atomic levels. For an ion with one electron

(e.g.,  $ns$  or  $np_{1/2}$  state) over the closed shells this splitting can be written in the form

$$\Delta E^{(a)} = \frac{\alpha(\alpha Z)^3 g_I}{n^3 m_p} \frac{2I+1}{(j+1)(2l+1)} \frac{1}{(1+\frac{m}{M})^3} \times \left[ A(\alpha Z)(1-\delta)(1-\varepsilon) + \frac{1}{Z}B(\alpha Z) + \frac{1}{Z^2}C(Z, \alpha Z) + x_{\text{rad}} \right]. \quad (3)$$

Here  $Z$  is the nuclear charge number,  $m_p$  and  $M$  are the proton and nuclear masses, respectively. Within the approximation of noninteracting electrons, where the contribution of the closed shells is neglected, the hyperfine splitting is explicitly determined by the quantum numbers of valence electron state  $a$ , which is characterized by the principal quantum number  $n$ , the angular momentum  $j$ , its projection  $m_j$ , and the parity  $l$ . A nucleus with spin  $I$  possesses a nuclear  $g$  factor  $g_I = \mu/\mu_N I$ , where  $\mu$  is the nuclear magnetic moment and  $\mu_N$  is the nuclear magneton.  $A(\alpha Z)$  is the one-electron relativistic factor,  $\delta$  and  $\varepsilon$  are, respectively, the corrections for distributions of the charge and magnetic moment over the nucleus; the functions  $B(\alpha Z)$  and  $C(Z, \alpha Z)$  determine the corrections for the electron-electron interaction of first and higher orders in  $1/Z$ , respectively;  $x_{\text{rad}}$  is the QED correction. These terms are subsequently described in the following subsections.

### A. One-electron contributions

The relativistic factor  $A(\alpha Z)$  corresponding to the point-like nucleus is known analytically [24]

$$A(\alpha Z) = \frac{n^3(2l+1)\kappa[2\kappa(\gamma+n_r)-N]}{N^4\gamma(4\gamma^2-1)}, \quad (4)$$

where  $n_r = n - |\kappa|$  is the radial quantum number,  $\kappa = (-1)^{j+l+1/2}(j+1/2)$ ,  $\gamma = \sqrt{\kappa^2 - (\alpha Z)^2}$ ,  $N = \sqrt{n_r^2 + 2n_r\gamma + \kappa^2}$ . The nuclear charge distribution correction  $\delta$  can be found either analytically [10, 25] or numerically by solving the Dirac equation with the Coulomb potential of the extended nucleus. In this work it is evaluated numerically employing the homogeneously-charged-sphere model for the nuclear charge distribution. In order to estimate the uncertainty due to the model dependence the Fermi model is used as well. The Bohr-Weisskopf correction  $\varepsilon$  originates from the spatial distribution of the magnetic moment inside the nucleus. For a rigorous treatment of this effect for low- $Z$  systems we refer to Ref. [26]. In the present work we restrict our consideration to models in which it can be accounted for by replacing the factor  $1/r^2$  in Eq. (2) by  $F(r)/r^2$ , where  $F(r)$  is the volume distribution function. For example, in case of the sphere model it reads

$$F(r) = \begin{cases} \left(\frac{r}{R_0}\right)^3, & r \leq R_0 \\ 1, & r > R_0 \end{cases}, \quad (5)$$

where  $R_0 = \sqrt{5/3} \langle r^2 \rangle^{1/2}$  is the radius of the sphere, and  $\langle r^2 \rangle^{1/2}$  is the charge root-mean-square radius of the nucleus. However, with the sphere model one can not always describe adequately the nuclear magnetization distribution. The approximation of the nuclear single-particle model is widely used for the evaluation of the Bohr-Weisskopf correction [10, 11, 12, 27, 28, 29, 30]. Within this model the nuclear magnetization is determined by the total angular momentum of the unpaired nucleon (proton or neutron). Accordingly, the nuclear  $g$  factor  $g_I$  is just the Landé factor of an extra nucleon, which is defined by the well-known formula

$$g_I = \mu/\mu_N I = \frac{1}{2} \left[ (g_L + g_S) + (g_L - g_S) \frac{L(L+1) - 3/4}{I(I+1)} \right], \quad (6)$$

where  $L$  is the nuclear orbital momentum,  $g_L$  and  $g_S$  are the orbital and spin  $g$  factors of the valence nucleon, respectively. In case of a valence proton  $g_L = 1$ , while for an extra neutron  $g_L = 0$ ;  $g_S$  is chosen such as to reproduce the experimental value of the nuclear magnetic moment  $\mu$  according to Eq. (6). For nuclei with odd or even nuclear charge numbers the role of the unpaired nucleon is either played by a proton or a neutron, respectively. In the framework of the nuclear single-particle model the radially symmetric distribution function  $F(r)$  has been derived in Refs. [27, 29, 30]. Here we neglect the contribution of the spin-orbit interaction and employ the homogeneous distribution for the radial part of the odd nucleon wavefunction inside the nucleus [10, 30]. In this approximation  $F(r)$  reads

$$F(r) = \left( \frac{r}{R_0} \right)^3 \left\{ 1 - 3 \ln \left( \frac{r}{R_0} \right) \frac{\mu_N}{\mu} \left[ -\frac{2I-1}{8(I+1)} g_S + \left( I - \frac{1}{2} \right) g_L \right] \right\}, \quad r \leq R_0, \quad (7)$$

for  $I = L + \frac{1}{2}$  and

$$F(r) = \left( \frac{r}{R_0} \right)^3 \left\{ 1 - 3 \ln \left( \frac{r}{R_0} \right) \frac{\mu_N}{\mu} \left[ \frac{2I+3}{8(I+1)} g_S + \frac{I(2I+3)}{2(I+1)} g_L \right] \right\}, \quad r \leq R_0, \quad (8)$$

for  $I = L - \frac{1}{2}$ . For  $r > R_0$  the distribution function  $F(r) = 1$ . In the case of  $^{14}\text{N}$  with  $I = 1$  we follow the work [11] and assume that the nuclear magnetization is determined by the odd proton and neutron. The corresponding formulas for  $\varepsilon$  were derived in Refs. [11, 31]. The uncertainty of the Bohr-Weisskopf correction is estimated as the maximum of two values: 50% of  $\varepsilon$  itself and the difference between  $\varepsilon$  obtained in single-particle and sphere nuclear models. As in our previous studies (see, e.g., the related discussion in Ref. [27]), the uncertainty obtained by this procedure must generally be considered only as the order of magnitude of the expected error bar. More accurate calculations of the Bohr-Weisskopf effect must be based on many-particle nuclear models and should include a more rigorous procedure for determination of the uncertainty. The

nuclear vector polarizability correction derived in Ref. [26] is assumed to contribute less than the uncertainty of  $\varepsilon$  indicated above.

Separating out the nuclear parameters and the nonrelativistic value of the hyperfine splitting one finds that the one-electron contributions considered above can be numerically evaluated in terms of a matrix element

$$A(\alpha Z)(1 - \delta)(1 - \varepsilon) = G_a \langle a|T_0|a \rangle \quad (9)$$

of the zero component  $T_0$  of the operator  $\mathbf{T}$  given by Eq. (2), multiplied by the magnetization distribution function  $F(r)$ . The wavefunction  $|a\rangle$  of the valence state, characterized by quantum numbers  $a = n, j, m_j$ , and  $l$ , is obtained as a solution of the Dirac equation with the potential of the extended nucleus. The multiplicative factor  $G_a$  reads

$$G_a = \frac{n^3(2l + 1)j(j + 1)}{2(\alpha Z)^3 m_j}. \quad (10)$$

## B. Many-electron contributions

Now we pass to the many-electron corrections. The term  $B(\alpha Z)/Z$  in Eq. (3) determines the interelectronic-interaction correction of the first order in  $1/Z$ . A rigorous QED treatment of this contribution can be carried out utilizing the two-time Green's function method [32]. To simplify the derivation of formal expressions, it is convenient to incorporate the core electrons as belonging to a redefined vacuum. This leads to merging the interelectronic-interaction correction of order  $1/Z$  with the one-loop radiative corrections. Such a treatment was applied previously in Refs. [33, 34]. The corresponding expression for the interelectronic-interaction correction reads

$$B(\alpha Z)/Z = 2G_a \sum_c \left\{ \sum_n^{\varepsilon_n \neq \varepsilon_a} \frac{\langle ac|I(0)|nc\rangle \langle n|T_0|a\rangle}{\varepsilon_a - \varepsilon_n} + \sum_n^{\varepsilon_n \neq \varepsilon_c} \frac{\langle ac|I(0)|an\rangle \langle n|T_0|c\rangle}{\varepsilon_c - \varepsilon_n} \right. \\ \left. - \sum_n^{\varepsilon_n \neq \varepsilon_a} \frac{\langle ac|I(\varepsilon_a - \varepsilon_c)|cn\rangle \langle n|T_0|a\rangle}{\varepsilon_a - \varepsilon_n} - \sum_n^{\varepsilon_n \neq \varepsilon_c} \frac{\langle ac|I(\varepsilon_a - \varepsilon_c)|na\rangle \langle n|T_0|c\rangle}{\varepsilon_c - \varepsilon_n} \right. \\ \left. - \frac{1}{2} [\langle a|T_0|a\rangle - \langle c|T_0|c\rangle] \langle ac|I'(\varepsilon_a - \varepsilon_c)|ca\rangle \right\}, \quad (11)$$

where  $\varepsilon_m$  are the one-electron energies,  $I(\omega) = e^2 \alpha^\mu \alpha^\nu D_{\mu\nu}(\omega)$ ,  $I'(\omega) = dI(\omega)/d\omega$ ,  $\alpha^\mu = (1, \boldsymbol{\alpha})$ , and  $D_{\mu\nu}(\omega)$  is the photon propagator. It should be noted that the total  $1/Z$  interelectronic-interaction correction given by Eq. (11) is gauge independent. We perform the calculation employ-

ing Coulomb and Feynman gauges for the photon propagator, thus receiving an accurate check of the gauge invariance of the results.

The interelectronic-interaction correction of higher orders  $C(Z, \alpha Z)/Z^2$  is calculated within the framework of the large-scale configuration-interaction method in the basis of Dirac-Fock-Sturm orbitals [35]. This method was successfully employed in our previous atomic calculations [36, 37, 38, 39, 40]. The interelectronic-interaction operator employed in the Dirac-Coulomb-Breit equation reads

$$V_{\text{int}} = \lambda\alpha \sum_{i<j} \left\{ \frac{1}{r_{ij}} - \frac{\boldsymbol{\alpha}_i \cdot \boldsymbol{\alpha}_j}{2r_{ij}} - \frac{(\boldsymbol{\alpha}_i \cdot \mathbf{r}_i)(\boldsymbol{\alpha}_j \cdot \mathbf{r}_j)}{2r_{ij}^3} \right\}, \quad (12)$$

where the sum runs over all electrons. A scaling parameter  $\lambda$  is introduced to separate terms of different order in  $1/Z$  from the numerical results with different  $\lambda$ . This representation allows us to perform the expansion in powers of  $\lambda$ . In this way, the higher-order term is written as

$$C(Z, \alpha Z)/Z^2 = G_a \left\{ \langle \Psi_\lambda(\gamma JM_J) | T_0 | \Psi_\lambda(\gamma JM_J) \rangle \Big|_{\lambda=1} - \langle \Psi_\lambda(\gamma JM_J) | T_0 | \Psi_\lambda(\gamma JM_J) \rangle \Big|_{\lambda=0} - \frac{d}{d\lambda} \langle \Psi_\lambda(\gamma JM_J) | T_0 | \Psi_\lambda(\gamma JM_J) \rangle \Big|_{\lambda=0} \right\}. \quad (13)$$

The many-electron wavefunction  $\Psi_\lambda(\gamma JM_J)$  is characterized by the total angular momentum  $J$ , its projection  $M_J$ , and the rest quantum numbers  $\gamma$ . The configuration-interaction matrix contains all single, double, and triple positive-energy excitations. Single-electron excitations to the negative-energy spectrum were accounted for in the many-electron wavefunction  $\Psi_\lambda(\gamma JM_J)$  employing perturbation theory.

The calculation of the interelectronic-interaction corrections  $B(\alpha Z)/Z$  and  $C(Z, \alpha Z)/Z^2$  is performed employing the homogeneously-charged-sphere model for the nuclear charge distribution and single-particle model for the nuclear magnetic moment distribution.

### C. One-loop radiative contribution

The one-loop radiative contribution  $x_{\text{rad}}$  appears as the sum of vacuum-polarization (VP) and self-energy (SE) corrections,  $x_{\text{rad}} = x_{\text{VP}} + x_{\text{SE}}$ , as depicted diagrammatically in Figs. 1 and 2, respectively. However, for the Li- and B-like ions along with the one-electron part the correction  $x_{\text{rad}}$  contains also the many-electron part. In order to account for many-electron effects we consider an effective spherically symmetric potential  $V_{\text{eff}}$  that partly takes into account the interelectronic

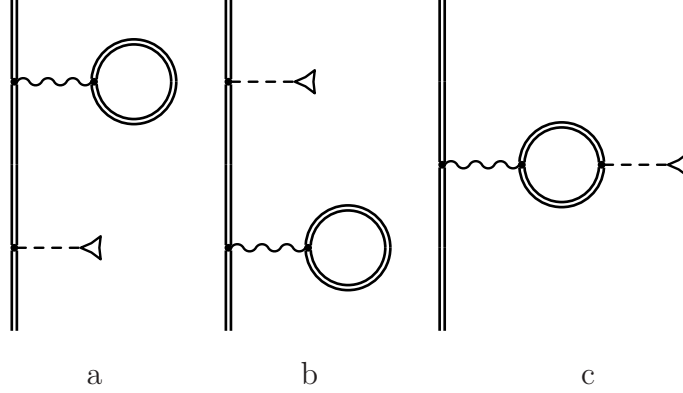


FIG. 1: Feynman diagrams representing the vacuum-polarization correction to the hyperfine splitting. The wavy line indicates the photon propagator and the double line indicates the bound-electron wavefunctions and propagators. The dashed line terminated with the triangle denotes the hyperfine interaction.

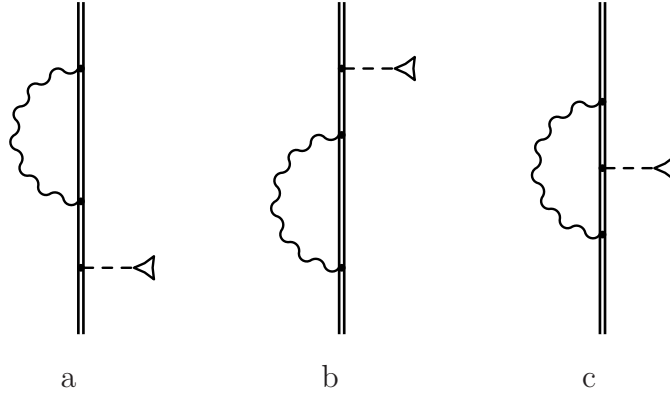


FIG. 2: Feynman diagrams representing the self-energy correction to the hyperfine splitting. Notations are the same as in Fig. 1.

interaction between the valence electron  $a$  and the core electrons  $c$ . This can be achieved by means of the Kohn-Sham screening potential derived within the density-functional theory [41]

$$V_{\text{eff}}(r) = V_{\text{nuc}}(r) + \alpha \int_0^\infty dr' \frac{1}{r'} \rho_t(r') - \frac{2\alpha}{3} \frac{\alpha}{r} \left( \frac{81}{32\pi^2} r \rho_t(r) \right)^{1/3}, \quad (14)$$

which we employed successfully in previous calculations [42, 43, 44, 45]. Here  $V_{\text{nuc}}$  is the potential of the extended nucleus and  $\rho_t$  denotes the total one-electron density. In order to estimate the sensitivity of the result on the specific choice of the screening potential we consider also the core-Hartree potential.

The VP correction  $x_{\text{VP}}$  is divided into the electric-loop part, Fig. 1 (a,b), which accounts for the VP correction to the scalar binding potential  $V_{\text{eff}}$ , and the magnetic-loop part, Fig. 1 (c), corre-



sponding to the VP-corrected hyperfine interaction potential. The expression for the electric-loop term Fig. 1 (a,b) reads

$$x_{\text{VP}}^{\text{el}} = 2G_a \sum_n^{\varepsilon_n \neq \varepsilon_a} \frac{\langle a|T_0|n\rangle \langle n|U_{\text{VP}}^{\text{el}}|a\rangle}{\varepsilon_a - \varepsilon_n}, \quad (15)$$

where  $U_{\text{VP}}^{\text{el}}$  represents the renormalized one-loop VP potential. It is divided into the Uehling and Wichmann-Kroll parts,  $U_{\text{VP}}^{\text{el}} = U_{\text{VP}}^{\text{Ue-el}} + U_{\text{VP}}^{\text{WK-el}}$ . The Uehling part can be evaluated according to the well-known equation

$$U_{\text{VP}}^{\text{Ue-el}}(r) = -\frac{2\alpha^2 Z}{3\pi} \int_1^\infty dt \frac{\sqrt{t^2 - 1}}{t^2} \left(1 + \frac{1}{2t^2}\right) \int d^3r' \frac{\rho_{\text{eff}}(\mathbf{r}')}{|\mathbf{r} - \mathbf{r}'|} e^{-2|\mathbf{r} - \mathbf{r}'|t}, \quad (16)$$

where the density  $\rho_{\text{eff}}$  is related to the effective binding potential  $V_{\text{eff}}$  [via the Poisson equation  $\Delta V_{\text{eff}}(\mathbf{r}) = 4\pi\alpha Z \rho_{\text{eff}}(\mathbf{r})$ ]. The Wichmann-Kroll part can be generated by summing up the partial-wave differences between the unrenormalized total VP potential and the unrenormalized Uehling term [46, 47]. In this work we employ the approximate formula for the Wichmann-Kroll electric-loop potential derived in Ref. [48]. The correction to the hyperfine splitting due to the magnetic loop  $x_{\text{VP}}^{\text{ml}}$  can be written in the form

$$x_{\text{VP}}^{\text{ml}} = G_a \langle a|U_{\text{VP}}^{\text{ml}}|a\rangle, \quad (17)$$

where  $U_{\text{VP}}^{\text{ml}}$  is the VP-corrected hyperfine potential  $T_0$ . It can be renormalized utilizing the same scheme as for the electric loop. For the distribution function  $F(r)$  corresponding to the sphere model (see Eq. (5)) we obtain the following analytical expression for the magnetic-loop Uehling term

$$U_{\text{VP}}^{\text{Ue-ml}}(r) = \frac{\alpha}{\pi} \frac{[\mathbf{n} \times \boldsymbol{\alpha}]_0}{r^2} \frac{3}{16R_0^3} \left\{ 4rR_0 \left[ \beta_1(R_0 + r) + \beta_1(|R_0 - r|) \right] + 2(R_0 + r) \beta_2(R_0 + r) \right. \\ \left. - 2|R_0 - r| \beta_2(|R_0 - r|) + \beta_3(R_0 + r) - \beta_3(|R_0 - r|) \right\}, \quad (18)$$

where the function  $\beta_n$  is defined as

$$\beta_n(r) = \frac{2}{3} \int_1^\infty dt \frac{\sqrt{t^2 - 1}}{t^{n+2}} \left(1 + \frac{1}{2t^2}\right) e^{-2tr}. \quad (19)$$

The contribution of the remaining Wichmann-Kroll magnetic-loop term is relatively small. For the case of the  $1s$  and  $2s$  states the values for the Wichmann-Kroll magnetic-loop term are taken from Ref. [22]. For  $2s$  we have also incorporated the screening effect, assuming that the screening

coefficient is the same as for the Uehling magnetic-loop term. For the  $2p_{1/2}$  state  $x_{\text{VP}}^{\text{WK-ml}}$  turns out to be smaller than the uncertainties assigned to the calculation.

Now let us turn to the evaluation of the SE correction. The formal expression can be derived by means of the two-time Green's function method [32]. The SE correction appears as the sum,  $x_{\text{SE}} = x_{\text{SE}}^{\text{irr}} + x_{\text{SE}}^{\text{red}} + x_{\text{SE}}^{\text{ver}}$ , of the irreducible  $x_{\text{SE}}^{\text{irr}}$ , reducible  $x_{\text{SE}}^{\text{red}}$ , and vertex  $x_{\text{SE}}^{\text{ver}}$  terms, respectively. The irreducible part, depicted in Fig. 2 (a,b) with the intermediate state energy  $\varepsilon_n \neq \varepsilon_a$ , is represented by the expression

$$x_{\text{SE}}^{\text{irr}} = 2G_a \sum_n^{\varepsilon_n \neq \varepsilon_a} \frac{\langle a|T_0|n\rangle \langle n|[\Sigma(\varepsilon_a) - \gamma^0 \delta m]|a\rangle}{\varepsilon_a - \varepsilon_n}, \quad (20)$$

where  $\delta m$  is the mass counter-term and  $\Sigma(\varepsilon)$  denotes the unrenormalized self-energy operator with matrix elements defined by

$$\langle a|\Sigma(\varepsilon)|b\rangle = \frac{i}{2\pi} \int_{-\infty}^{\infty} d\omega \sum_n \frac{\langle an|I(\omega)|nb\rangle}{\varepsilon - \omega - \varepsilon_n(1 - i0)}. \quad (21)$$

Accordingly, the irreducible contribution can be written as nondiagonal matrix element of the self-energy operator. Thus, the renormalization scheme developed for the first-order self-energy correction can be also applied in this case (see, e.g., Refs. [49, 50, 51]). Only a slight extension of the corresponding formulas for the case of a nondiagonal matrix element is needed.

The expression for the reducible term is given by

$$x_{\text{SE}}^{\text{red}} = G_a \langle a|\frac{d\Sigma(\varepsilon)}{d\varepsilon}\Big|_{\varepsilon=\varepsilon_a}|a\rangle \langle a|T_0|a\rangle, \quad (22)$$

while the vertex part, Fig. 2 (c), reads

$$x_{\text{SE}}^{\text{ver}} = G_a \frac{i}{2\pi} \int_{-\infty}^{\infty} d\omega \sum_{n_1 n_2} \frac{\langle an_2|I(\omega)|n_1a\rangle \langle n_1|T_0|n_2\rangle}{(\varepsilon_a - \omega - \varepsilon_{n_1}(1 - i0))(\varepsilon_a - \omega - \varepsilon_{n_2}(1 - i0))}. \quad (23)$$

Both reducible and vertex terms are ultraviolet-divergent. In order to isolate the divergencies in a covariant way, we separate out the zero-potential terms in which bound electron propagators are replaced by free propagators. The sum of the latter terms for the reducible and the vertex part is denoted by  $x_{\text{SE}}^{\text{vr}(0)} = x_{\text{SE}}^{\text{red}(0)} + x_{\text{SE}}^{\text{ver}(0)}$ . Their evaluation is performed in momentum space, where the ultraviolet divergencies can be canceled in a standard way. The remaining part of the reducible and the vertex contribution  $x_{\text{SE}}^{\text{vr}(1+)}$  is ultraviolet finite. However, we note that the term with  $\varepsilon_{n_1} = \varepsilon_{n_2} = \varepsilon_a$  in Eq. (23) involves an infrared divergency, which is canceled by the corresponding term of the reducible contribution. Performing the integration over the energy of the

virtual photon in these terms analytically we explicitly achieve the finite result in the sum of the reducible and vertex contributions. The remaining part of the many-potential term  $x_{\text{SE}}^{\text{vr}(1+)}$  is infrared finite, and can be calculated in coordinate space by means of a point-by-point subtraction of the corresponding contributions with free propagators inside of the self-energy loop. Angular integration and summation over intermediate angular momentum projections is carried out in a standard way [51]. The evaluation of the many-potential terms performed in the coordinate space involves an infinite summation over the angular-momentum quantum number  $\kappa$  of intermediate states. This sum was extended up to  $|\kappa_{\text{max}}| = 10$  and the remaining part of the sum is estimated by a least-square inverse-polynomial fitting. One also observes that the results of the radial integration converge better, when an extended model for the magnetization distribution is employed. In our calculations of the radiative corrections we have utilized the sphere model for the magnetic moment distribution function  $F(r)$ .

### III. NUMERICAL RESULTS

Now let us pass to the presentation of the numerical procedure and the results for H-, Li-, and B-like sequences. The infinite summations over the complete spectrum of the Dirac equation involved in the numerical evaluations are performed employing the finite-basis set approach. The B-splines basis set was constructed utilizing the dual kinetic balance approach [52]. The latter treats large and small components on equal footing and respects the charge conjugation symmetry. As a consequence no unphysical spurious states appear and moreover, it improves the convergence properties and the accuracy considerably. The values of the nuclear root-mean-square radii are taken from the tabulation [53]. The root-mean-square radius, in particular, for the  $^{33}\text{S}$  isotope is assumed to be the average of the values given for even isotopes  $^{32}\text{S}$  and  $^{34}\text{S}$ , respectively. Empirical data for the nuclear properties: spin  $I$ , parity  $\pi$ , and magnetic moment  $\mu/\mu_N$  are taken from Ref. [54]. All these values are also compiled in Table I. We indicate the uncertainties assigned to the nuclear magnetic moments only if they exceed the level of  $10^{-5}$  in the relative units. One has to note here, that the magnetic moment values obtained via the nuclear magnetic resonance technique do not usually account for the chemical shift [55], which is of the order  $10^{-3} - 10^{-4}$  or sometimes even larger.

### A. H-like ions

The individual contributions to the hyperfine splitting for the light H-like ions are presented in Table I. The values obtained for the radiative corrections  $x_{\text{SE}}$  and  $x_{\text{VP}}$  are in good agreement with the most accurate nonperturbative results [22] based on the Coulomb-Dirac Green function. The slight difference is explained by the finite-nuclear-size effects accounted for in the present work. The latter is especially important for the evaluation of the specific difference between H- and Li-like hyperfine splitting values, where the QED corrections have to be calculated within the same nuclear model. As one can see from the table the main uncertainty originates from the Bohr-Weisskopf correction  $\varepsilon$ . In Table II the predictions for the total transition energies  $\Delta E^{(1s)}$  are compared with the results of previous calculations [11, 13]. Deviations between our results and those reported in Ref. [13] arise from the different treatment of the Bohr-Weisskopf effect. In work [13] the simple spherical model for the magnetization distribution was employed. Theoretical values for the total transition energies  $\Delta E^{(1s)}$  and wavelengths  $\lambda^{(1s)}$  are presented in Table X below.

### B. Li-like ions

The consideration of Li-like ions we start with the results for the screened radiative corrections  $x_{\text{SE}}$  and  $x_{\text{VP}}$ . The one-loop QED correction is conveniently represented in terms of the function  $D_{\text{rad}}$  defined as

$$x_{\text{rad}} = \frac{\alpha}{\pi} D_{\text{rad}}. \quad (24)$$

In Tables III and IV the numerical results for individual contributions to the self-energy ( $D_{\text{SE}}$ ) and vacuum-polarization ( $D_{\text{VP}}$ ) corrections are presented, respectively, for  $Z = 10, 15, 20, 25$ .

Table V displays the individual contributions to the hyperfine splitting of the light Li-like ions. As in the case of H-like ions the main uncertainty originates from the Bohr-Weisskopf correction  $\varepsilon$ . Earlier calculations on the hyperfine structure of light Li-like ions [11, 12, 13] account for the radiative correction on the basis of analytical expansion with respect to  $\alpha Z$ . Here we have performed exact (to all orders in  $\alpha Z$ ) evaluations of one-loop QED corrections with an effective screening potential and with a nuclear vector potential involving an extended magnetization distribution. As compared to the results of works [11, 12], several additional improvements have been achieved:

TABLE I: Individual contributions to the ground-state hyperfine splitting of the hydrogenlike ions.

Ion	$I^\pi$	$\mu/\mu_N$	$\langle r^2 \rangle^{1/2}$	$A(\alpha Z)$	$\delta$	$\varepsilon$	$x_{SE}$	$x_{VP}$
$^{14}\text{N}^{6+}$	1+	0.40376	2.5579	1.00393	0.00067(3)	-0.00004(28)	0.00009	0.00028
$^{15}\text{N}^{6+}$	$\frac{1}{2}-$	-0.28319	2.6061	1.00393	0.00068(3)	0.00114(88)	0.00009	0.00028
$^{17}\text{O}^{7+}$	$\frac{5}{2}+$	-1.8938(1)	2.6953	1.00514	0.00081(3)	0.00033(17)	-0.00006	0.00032
$^{19}\text{F}^{8+}$	$\frac{1}{2}+$	2.6289	2.8976	1.00651	0.00099(3)	0.00036(18)	-0.00022	0.00036
$^{21}\text{Ne}^{9+}$	$\frac{3}{2}+$	-0.66180(1)	2.9672	1.00805	0.00113(4)	0.00058(29)	-0.00037	0.00040
$^{23}\text{Na}^{10+}$	$\frac{3}{2}+$	2.2175	2.9936	1.00975	0.00127(4)	0.00035(18)	-0.00053	0.00044
$^{25}\text{Mg}^{11+}$	$\frac{5}{2}+$	-0.85545(8)	3.0280	1.01163	0.00141(4)	0.00057(29)	-0.00068	0.00049
$^{27}\text{Al}^{12+}$	$\frac{5}{2}+$	3.6415	3.0605	1.01367	0.00156(5)	0.00048(24)	-0.00084	0.00053
$^{29}\text{Si}^{13+}$	$\frac{1}{2}+$	-0.55529(3)	3.1168	1.01589	0.00173(5)	0.00063(31)	-0.00099	0.00058
$^{31}\text{P}^{14+}$	$\frac{1}{2}+$	1.1316	3.1888	1.01828	0.00191(5)	0.00069(35)	-0.00115	0.00062
$^{33}\text{S}^{15+}$	$\frac{3}{2}+$	0.64382	3.2727	1.02085	0.00212(6)	0.00106(53)	-0.00130	0.00067
$^{35}\text{Cl}^{16+}$	$\frac{3}{2}+$	0.82187	3.3652	1.02360	0.00234(6)	-0.00026(110)	-0.00146	0.00071
$^{37}\text{Cl}^{16+}$	$\frac{3}{2}+$	0.68412	3.3840	1.02360	0.00235(6)	-0.00055(140)	-0.00146	0.00071
$^{39}\text{K}^{18+}$	$\frac{3}{2}+$	0.39147	3.4346	1.02964	0.00274(6)	-0.0021(31)	-0.00177	0.00081
$^{41}\text{K}^{18+}$	$\frac{3}{2}+$	0.21487	3.4514	1.02964	0.00275(6)	-0.0050(60)	-0.00177	0.00081
$^{43}\text{Ca}^{19+}$	$\frac{7}{2}-$	-1.3176	3.4928	1.03294	0.00297(7)	0.00119(60)	-0.00193	0.00086
$^{45}\text{Sc}^{20+}$	$\frac{7}{2}-$	4.7565	3.5443	1.03644	0.00320(7)	0.00092(46)	-0.00208	0.00091
$^{47}\text{Ti}^{21+}$	$\frac{5}{2}-$	-0.78848(1)	3.5944	1.04012	0.00345(7)	0.00160(80)	-0.00224	0.00096
$^{49}\text{Ti}^{21+}$	$\frac{7}{2}-$	-1.1042	3.5735	1.04012	0.00343(7)	0.00137(69)	-0.00224	0.00096
$^{51}\text{V}^{22+}$	$\frac{7}{2}-$	5.1487	3.5994	1.04401	0.00367(8)	0.00107(54)	-0.00240	0.00101
$^{53}\text{Cr}^{23+}$	$\frac{3}{2}-$	-0.47454(3)	3.6588	1.04810	0.00395(8)	0.00149(75)	-0.00256	0.00106
$^{55}\text{Mn}^{24+}$	$\frac{5}{2}-$	3.4687	3.7057	1.05239	0.00423(8)	0.00109(54)	-0.00272	0.00111
$^{57}\text{Fe}^{25+}$	$\frac{1}{2}-$	0.090623	3.7534	1.05689	0.00453(9)	0.00279(140)	-0.00289	0.00117
$^{59}\text{Co}^{26+}$	$\frac{7}{2}-$	4.627(9)	3.7875	1.06161	0.00483(9)	0.00133(66)	-0.00305	0.00123
$^{61}\text{Ni}^{27+}$	$\frac{3}{2}-$	-0.75002(4)	3.8221	1.06655	0.00514(9)	0.00191(95)	-0.00322	0.00128

 TABLE II: Comparison of the ground-state hyperfine splitting  $\Delta E^{(1s)}$  of H-like ions between different theoretical calculations. The values of the energies are given in meV.

Ion	$\mu/\mu_N$	this work	[11]	[13]
$^{14}\text{N}^{6+}$	0.40376	0.21936(6)	0.21937(4)	0.21931
$^{27}\text{Al}^{12+}$	3.6415	10.215(2)		10.215
$^{45}\text{Sc}^{20+}$	4.7565	54.613(25)		54.601
$^{57}\text{Fe}^{25+}$	0.090623	3.5109(49)		3.5152

the interelectronic-interaction corrections  $B(\alpha Z)/Z$  and  $C(Z, \alpha Z)/Z^2$  have been calculated taking into account explicitly the extended nuclear charge and magnetic moment distribution effects, moreover, the term  $C(Z, \alpha Z)/Z^2$  has now been evaluated within the framework of the relativistic CI-DFS method. The latter is especially important for ions of the higher  $Z$  region. The remaining one-electron corrections  $A(\alpha Z)$ ,  $\delta$ , and  $\varepsilon$  coincide with the results of works [11, 12]. The recoil effect for Li-like ions is partly accounted for by a factor  $(1 + m/M)^{-3}$  in Eq. (3). However, addi-

TABLE III: Individual contributions to the screened self-energy correction for the ground-state hyperfine structure of the lithiumlike ions, in units of the function  $D_{SE}$ .

$Z$	$D_{SE}^{irr}$	$D_{SE}^{vr(0)}$	$D_{SE}^{vr(1+)}$	$D_{SE}$
10	-0.161	2.723	-2.661	-0.100
15	-0.296	2.685	-2.760	-0.372
20	-0.443	2.543	-2.772	-0.672
25	-0.602	2.380	-2.775	-0.999

TABLE IV: Individual contributions to the screened vacuum-polarization correction for the ground-state hyperfine structure of the lithiumlike ions, in units of the function  $D_{VP}$ .

$Z$	$D_{VP}^{Ue-el}$	$D_{VP}^{Ue-ml}$	$D_{VP}^{WK-el}$	$D_{VP}^{WK-ml}$	$D_{VP}$
10	0.067	0.058	-0.000037	-0.00020	0.125
15	0.119	0.098	-0.00015	-0.00076	0.216
20	0.178	0.140	-0.00039	-0.0020	0.316
25	0.247	0.186	-0.00083	-0.0041	0.428

tional contributions arising from the specific mass shift and spin-orbit recoil corrections [56] are significantly smaller than the uncertainty assigned for the Bohr-Weisskopf correction.

In Table VI results for the total ground-state hyperfine splitting values of lithiumlike ions  $\Delta E^{(2s)}$  of different theoretical calculations are compared. In addition the experimental value of a recent measurement of the hyperfine splitting of lithiumlike  $^{45}\text{Sc}^{18+}$  ion, performed by resolving the  $2s$  hyperfine structure in the dielectronic recombination spectrum [57], is given as well. The deviations between our results and values reported in Ref. [13] are mainly determined by interelectronic-interaction effects. The total theoretical values of the energies  $\Delta E^{(2s)}$  and wavelengths  $\lambda^{(2s)}$  are reported in Table X.

### C. B-like ions

Let us now turn to boronlike ions. The corresponding screened radiative corrections  $x_{SE}$  and  $x_{VP}$  expressed in terms of the functions  $D_{SE}$  and  $D_{VP}$  defined by Eq. (24) are presented in Tables VII and VIII, respectively. The uncalculated Wichmann-Kroll contribution of the magnetic-loop  $D_{VP}^{WK-ml}$  is of the same order as the corresponding electric-loop term  $D_{VP}^{WK-el}$ . As can be

TABLE V: Individual contributions to the ground-state hyperfine splitting of the lithiumlike ions. The values of the nuclear parameters are the same as in Table I.

Ion	$A(\alpha Z)$	$\delta$	$\varepsilon$	$x_{SE}$	$x_{VP}$	$B(\alpha Z)/Z$	$C(Z, \alpha Z)/Z^2$
$^{14}\text{N}^{4+}$	1.00557	0.00067(3)	-0.00004(28)	0.00008	0.00017	-0.38146	0.01800
$^{15}\text{N}^{4+}$	1.00557	0.00068(3)	0.00114(88)	0.00008	0.00017	-0.38101	0.01798
$^{17}\text{O}^{5+}$	1.00728	0.00081(3)	0.00033(17)	-0.00001	0.00021	-0.33424	0.01387
$^{19}\text{F}^{6+}$	1.00923	0.00099(3)	0.00036(18)	-0.00012	0.00025	-0.29767	0.01104
$^{21}\text{Ne}^{7+}$	1.01142	0.00113(4)	0.00058(29)	-0.00023	0.00029	-0.26845	0.00900
$^{23}\text{Na}^{8+}$	1.01384	0.00127(4)	0.00035(18)	-0.00035	0.00033	-0.24471	0.00749
$^{25}\text{Mg}^{9+}$	1.01650	0.00141(4)	0.00057(29)	-0.00047	0.00037	-0.22488	0.00634
$^{27}\text{Al}^{10+}$	1.01941	0.00156(5)	0.00048(24)	-0.00060	0.00042	-0.20823	0.00544
$^{29}\text{Si}^{11+}$	1.02257	0.00173(5)	0.00063(32)	-0.00073	0.00046	-0.19395	0.00473
$^{31}\text{P}^{12+}$	1.02597	0.00192(5)	0.00070(35)	-0.00086	0.00050	-0.18164	0.00415
$^{33}\text{S}^{13+}$	1.02963	0.00212(6)	0.00107(53)	-0.00100	0.00055	-0.17086	0.00368
$^{35}\text{Cl}^{14+}$	1.03355	0.00235(6)	-0.00026(111)	-0.00113	0.00059	-0.16166	0.00329
$^{37}\text{Cl}^{14+}$	1.03355	0.00236(6)	-0.00055(140)	-0.00113	0.00059	-0.16171	0.00329
$^{39}\text{K}^{16+}$	1.04219	0.00275(6)	-0.0021(31)	-0.00142	0.00069	-0.14619	0.00268
$^{41}\text{K}^{16+}$	1.04219	0.00276(6)	-0.0050(60)	-0.00142	0.00069	-0.14661	0.00269
$^{43}\text{Ca}^{17+}$	1.04691	0.00298(7)	0.00120(60)	-0.00156	0.00073	-0.13908	0.00244
$^{45}\text{Sc}^{18+}$	1.05191	0.00322(7)	0.00092(46)	-0.00171	0.00078	-0.13316	0.00223
$^{47}\text{Ti}^{19+}$	1.05719	0.00347(7)	0.00161(81)	-0.00186	0.00083	-0.12769	0.00205
$^{49}\text{Ti}^{19+}$	1.05719	0.00345(7)	0.00138(69)	-0.00186	0.00083	-0.12772	0.00205
$^{51}\text{V}^{20+}$	1.06277	0.00369(8)	0.00108(54)	-0.00201	0.00089	-0.12288	0.00190
$^{53}\text{Cr}^{21+}$	1.06864	0.00398(8)	0.00151(75)	-0.00216	0.00094	-0.11840	0.00176
$^{55}\text{Mn}^{22+}$	1.07481	0.00427(8)	0.00110(55)	-0.00232	0.00099	-0.11440	0.00164
$^{57}\text{Fe}^{23+}$	1.08130	0.00457(9)	0.00282(141)	-0.00248	0.00105	-0.11050	0.00154
$^{59}\text{Co}^{24+}$	1.08811	0.00487(9)	0.00134(67)	-0.00264	0.00111	-0.10728	0.00144
$^{61}\text{Ni}^{25+}$	1.09524	0.00519(9)	0.00193(96)	-0.00281	0.00117	-0.10410	0.00136

TABLE VI: Comparison of the ground-state hyperfine splitting  $\Delta E^{(2s)}$  of Li-like ions between different theoretical calculations and experimental data. The values of the energies are given in meV.

Ion	$\mu/\mu_N$	this work	[12]	[13]	Exp. [57]
$^{14}\text{N}^{4+}$	0.40376	0.017532(8)	0.017532(10)	0.017667	
$^{27}\text{Al}^{10+}$	3.6415	1.0283(3)	1.0281(6)	1.0326	
$^{45}\text{Sc}^{18+}$	4.7565	6.0631(32)	6.063(6)	6.0767	6.20(8)
$^{57}\text{Fe}^{23+}$	0.090623	0.40345(64)	0.4036(7)	0.40470	

seen from Table VIII, the values of the correction  $D_{VP}^{WK-el}$  are smaller than the uncertainty of the self-energy contribution  $D_{SE}$ . Therefore, in the case of light B-like ions one can neglect the contributions of the Wichmann-Kroll terms.

In Table IX numerical results for the individual contributions to the hyperfine splitting in light B-like ions are displayed. In contrast to the hydrogen- and lithiumlike sequences, where the va-

TABLE VII: Individual contributions to the screened self-energy correction for the ground-state hyperfine splitting of the boronlike ions, in units of the function  $D_{SE}$ .

$Z$	$D_{SE}^{\text{irr}}$	$D_{SE}^{\text{vr}(0)}$	$D_{SE}^{\text{vr}(1+)}$	$D_{SE}$
10	0.000	0.630	-0.521	0.109
15	-0.001	0.742	-0.608	0.132
20	-0.002	0.781	-0.648	0.131
25	-0.005	0.788	-0.666	0.117

TABLE VIII: Individual contributions to the screened vacuum-polarization correction for the ground-state hyperfine splitting of the boronlike ions, in units of the function  $D_{VP}$ .

$Z$	$D_{VP}^{\text{Ue-el}}$	$D_{VP}^{\text{Ue-ml}}$	$D_{VP}^{\text{WK-el}}$	$D_{VP}$
10	0.00011	0.00066	-0.000000084	0.00078
15	0.00059	0.0023	-0.00000097	0.0029
20	0.0018	0.0052	-0.0000051	0.0069
25	0.0041	0.0096	-0.000018	0.0137

lence electrons are in the  $s$  states, boronlike ions have the valence electron in the  $p_{1/2}$  state; its electron density vanishes at the origin. Since the nuclear structure corrections  $\delta$  and  $\varepsilon$  arise from the nuclear region, these contributions are much smaller in the B-like ions than in corresponding H- and Li-like ions. For the uncertainty of the radiative correction we prefer a conservative estimation as the difference of QED corrections calculated with and without screening potential. This uncertainty dominates for ions in the low- $Z$  region. Evaluation of the screened radiative correction within the rigorous QED approach is presently underway. For high- $Z$  ions the total theoretical uncertainty is mainly determined by the frequency-dependent (QED) contribution in the higher-order interelectronic-interaction term  $C(Z, \alpha Z)/Z^2$ , which is estimated to be of the order  $(\alpha Z)^3 C(Z, \alpha Z)/Z^2$ . In Table X the total theoretical values of the energies  $\Delta E^{(2p_{1/2})}$  and wavelengths  $\lambda^{(2p_{1/2})}$  are reported. The recoil correction is accounted for by a factor  $(1 + m/M)^{-3}$  in Eq. (3) with 100% uncertainty, caused by uncalculated specific mass shift and spin-orbit recoil corrections [56].



TABLE IX: Individual contributions to the ground-state hyperfine splitting of the boronlike ions. The values of the nuclear parameters are the same as in Table I.

Ion	$A(\alpha Z)$	$\delta$	$\varepsilon$	$x_{\text{rad}}$	$B(\alpha Z)/Z$	$C(Z, \alpha Z)/Z^2$
$^{14}\text{N}^{2+}$	1.00513	0.000001	0.000000(1)	0.00017(37)	-0.82166	0.15006(2)
$^{15}\text{N}^{2+}$	1.00513	0.000001	0.000002(2)	0.00017(37)	-0.82166	0.15006(2)
$^{17}\text{O}^{3+}$	1.00671	0.000002	0.000001	0.00020(33)	-0.72061	0.11479(2)
$^{19}\text{F}^{4+}$	1.00850	0.000002	0.000001(1)	0.00023(29)	-0.64222	0.09083(3)
$^{21}\text{Ne}^{5+}$	1.01052	0.000003	0.000002(1)	0.00025(26)	-0.57969	0.07381(3)
$^{23}\text{Na}^{6+}$	1.01275	0.000005	0.000002(1)	0.00027(24)	-0.52869	0.06128(3)
$^{25}\text{Mg}^{7+}$	1.01520	0.000006	0.000003(1)	0.00029(21)	-0.48635	0.05179(3)
$^{27}\text{Al}^{8+}$	1.01788	0.000008	0.000003(1)	0.00030(19)	-0.45068	0.04443(4)
$^{29}\text{Si}^{9+}$	1.02078	0.000010	0.000004(2)	0.00031(17)	-0.42023	0.03860(4)
$^{31}\text{P}^{10+}$	1.02392	0.000013	0.000005(3)	0.00031(16)	-0.39398	0.03391(4)
$^{33}\text{S}^{11+}$	1.02728	0.000016	0.000009(5)	0.00032(14)	-0.37113	0.03008(5)
$^{35}\text{Cl}^{12+}$	1.03089	0.000021(1)	-0.000003(11)	0.00032(13)	-0.35110	0.02691(5)
$^{37}\text{Cl}^{12+}$	1.03089	0.000021(1)	-0.000006(14)	0.00032(13)	-0.35110	0.02691(5)
$^{39}\text{K}^{14+}$	1.03882	0.000030(1)	-0.000026(38)	0.00032(10)	-0.31768	0.02203(6)
$^{41}\text{K}^{14+}$	1.03882	0.000030(1)	-0.000062(74)	0.00032(10)	-0.31770	0.02203(6)
$^{43}\text{Ca}^{15+}$	1.04316	0.000036(1)	0.000016(8)	0.00032(9)	-0.30363	0.02012(6)
$^{45}\text{Sc}^{16+}$	1.04775	0.000043(1)	0.000014(7)	0.00032(8)	-0.29103	0.01849(7)
$^{47}\text{Ti}^{17+}$	1.05260	0.000051(1)	0.000026(13)	0.00032(7)	-0.27967	0.01708(7)
$^{49}\text{Ti}^{17+}$	1.05260	0.000051(1)	0.000023(11)	0.00032(7)	-0.27967	0.01708(7)
$^{51}\text{V}^{18+}$	1.05772	0.000060(1)	0.000019(10)	0.00031(6)	-0.26941	0.01585(7)
$^{53}\text{Cr}^{19+}$	1.06311	0.000070(1)	0.000029(15)	0.00031(5)	-0.26010	0.01477(8)
$^{55}\text{Mn}^{20+}$	1.06877	0.000082(2)	0.000023(12)	0.00030(5)	-0.25163	0.01383(8)
$^{57}\text{Fe}^{21+}$	1.07472	0.000095(2)	0.000064(32)	0.00030(4)	-0.24390(1)	0.01300(9)
$^{59}\text{Co}^{22+}$	1.08096	0.000109(2)	0.000033(16)	0.00029(3)	-0.23685(1)	0.01226(9)
$^{61}\text{Ni}^{23+}$	1.08749	0.000125(2)	0.000051(25)	0.00029(2)	-0.23039(1)	0.01160(10)

#### IV. DISCUSSION

Predictions for the total energies  $\Delta E^{(a)}$  and wavelengths  $\lambda^{(a)}$  of the transitions between the ground-state hyperfine splitting components of the light H-, Li-, and B-like ions are given in Table X. Due to the discrepancies in the experimental data for nuclear magnetic moments  $\mu$  for some ions we have evaluated transition energies and wavelengths for all values of  $\mu$  reported in Ref. [54]. The values of the nuclear spin and parity, and the root-mean-square radii are the same as in Table I. In the parentheses the uncertainty of the presented results is indicated. For  $1s$  and  $2s$  states it is mainly due to the Bohr-Weisskopf effect and must generally be considered as the order of magnitude of the expected error bar. For some ions we give also a second value for the uncertainty, which corresponds to the uncertainty of the nuclear magnetic moment. The values

TABLE X: The energies  $\Delta E^{(a)}$  (meV) and wavelengths  $\lambda^{(a)}$  (cm) of the transitions between the ground-state hyperfine splitting of the H-, Li-, and B-like ions.

Nucleus	$\mu/\mu_N$	$\Delta E^{(1s)}$	$\lambda^{(1s)}$	$\Delta E^{(2s)}$	$\lambda^{(2s)}$	$\Delta E^{(2p_{1/2})}$	$\lambda^{(2p_{1/2})}$
<sup>14</sup> N	0.40376	0.21936(6)	0.56521(16)	0.017532(8)	7.0720(31)	0.0030389(34)	40.799(46)
<sup>15</sup> N	-0.28319	0.20490(18)	0.60510(53)	0.016376(23)	7.5711(105)	0.0028419(32)	43.627(49)
<sup>17</sup> O	-1.8938(1)	1.2294(2)(1)	0.10085(2)(1)	0.10497(3)(1)	1.1811(3)(1)	0.020459(17)(1)	6.0602(50)(3)
<sup>19</sup> F	2.6289	4.0541(7)	0.030582(6)	0.36364(9)	0.34095(9)	0.076848(49)	1.6134(10)
<sup>21</sup> Ne	-0.66180(1)	0.93432(27)(1)	0.13270(4)	0.087074(34)(1)	1.4239(6)	0.019531(10)	6.3481(33)(1)
<sup>23</sup> Na	2.2175	4.1738(8)	0.029705(5)	0.40110(9)	0.30911(7)	0.094130(42)	1.3172(6)
	2.2177	4.1742(8)	0.029703(5)	0.40113(9)	0.30909(7)	0.094138(42)	1.3170(6)
<sup>25</sup> Mg	-0.85545(8)	1.8840(5)(2)	0.065809(19)(6)	0.18567(7)(2)	0.66777(25)(6)	0.045176(17)(4)	2.7445(10)(3)
<sup>27</sup> Al	3.6415	10.215(2)	0.012137(3)	1.0283(3)	0.12058(4)	0.25755(8)	0.48140(16)
<sup>29</sup> Si	-0.55529(3)	3.2484(10)(2)	0.038168(12)(2)	0.33293(13)(2)	0.37240(15)(2)	0.085431(24)(5)	1.4513(4)(1)
<sup>31</sup> P	1.1316	8.1582(29)	0.015198(5)	0.84933(36)	0.14598(6)	0.22240(6)	0.55748(14)
<sup>33</sup> S	0.64382	3.7624(20)	0.032954(18)	0.39711(25)	0.31221(20)	0.10583(2)	1.1716(3)
<sup>35</sup> Cl	0.82187	5.7821(64)	0.021443(24)	0.61780(81)	0.20069(26)	0.16687(3)	0.74298(15)
<sup>37</sup> Cl	0.68412	4.8143(67)	0.025753(36)	0.51439(85)	0.24103(40)	0.13891(3)	0.89258(18)
<sup>39</sup> K	0.39147	3.873(12)	0.03202(10)	0.4225(15)	0.2934(11)	0.11670(2)	1.0625(2)
	0.39151	3.873(12)	0.03201(10)	0.4226(15)	0.2934(11)	0.11671(2)	1.0624(2)
<sup>41</sup> K	0.21487	2.132(13)	0.05816(35)	0.2326(16)	0.5331(37)	0.064053(12)	1.9356(4)
	0.21489	2.132(13)	0.05816(35)	0.2326(16)	0.5330(37)	0.064059(12)	1.9355(4)
<sup>43</sup> Ca	-1.3176	13.025(8)	0.0095191(57)	1.4340(10)	0.086460(60)	0.40134(6)	0.30892(5)
<sup>45</sup> Sc	4.7565	54.613(25)	0.0022702(11)	6.0631(32)	0.020449(11)	1.7115(2)	0.072440(10)
<sup>47</sup> Ti	-0.78848(1)	10.957(9)	0.011316(9)	1.2259(11)	0.10114(9)	0.34905(5)	0.35520(5)
<sup>49</sup> Ti	-1.1042	14.617(10)	0.0084821(59)	1.6355(13)	0.075810(60)	0.46554(6)	0.26632(3)
<sup>51</sup> V	5.1487	78.168(42)	0.0015861(9)	8.8099(54)	0.014073(9)	2.5248(3)	0.049107(6)
<sup>53</sup> Cr	-0.47454(3)	9.5797(72)(6)	0.012942(10)(1)	1.0871(9)(1)	0.11406(10)(1)	0.31367(4)(2)	0.39527(5)(2)
<sup>55</sup> Mn	3.4687	71.525(39)	0.0017334(9)	8.1688(50)	0.015178(9)	2.3699(3)	0.052315(6)
	3.4532(13)	71.206(39)(27)	0.0017412(9)(7)	8.1323(50)(31)	0.015246(9)(6)	2.3594(3)(9)	0.052550(6)(20)
<sup>57</sup> Fe	0.090623	3.5109(49)	0.035314(50)	0.40345(64)	0.30731(49)	0.11787(1)	1.0519(1)
	0.090764	3.5164(49)	0.035259(50)	0.40408(64)	0.30683(48)	0.11805(1)	1.0503(1)
	0.09044(7)	3.5038(49)(27)	0.035386(50)(27)	0.40264(64)(31)	0.30793(49)(24)	0.11763(1)(9)	1.0540(1)(8)
<sup>59</sup> Co	4.627(9)	115.35(8)(22)	0.0010749(7)(21)	13.334(10)(26)	0.0092987(69)(181)	3.9084(5)(76)	0.031722(4)(62)
<sup>61</sup> Ni	-0.75002(4)	24.418(23)(1)	0.0050777(49)(3)	2.8385(30)(2)	0.043680(47)(2)	0.83617(10)(4)	0.14828(2)(1)

for lithiumlike <sup>45</sup>Sc<sup>18+</sup> and boronlike <sup>45</sup>Sc<sup>16+</sup>, <sup>57</sup>Fe<sup>21+</sup> ions coincide with our previous results [43, 44, 45]. Due to the lack of experimental data one can not make a detailed comparison for the ions under consideration.

Table X shows excellent accuracy for the values of the hyperfine splitting of H-, Li- and B-like ions. For the H- and Li-like ions the limitation of the total accuracy is set by the Bohr-Weisskopf correction. However, this uncertainty can be considerably reduced in the specific difference of the

ground-state hyperfine structure values of H- and Li-like ions with the same nucleus [9]

$$\Delta' E = \Delta E^{(2s)} - \xi \Delta E^{(1s)}. \quad (25)$$

The parameter  $\xi$  has to be chosen to cancel the Bohr-Weisskopf correction

$$\xi = \frac{1}{8} \frac{A^{(2s)}(\alpha Z)(1 - \delta^{(2s)})}{A^{(1s)}(\alpha Z)(1 - \delta^{(1s)})} f(\alpha Z). \quad (26)$$

The function  $f(\alpha Z)$  is defined by the ratio of the Bohr-Weisskopf corrections

$$f(\alpha Z) = \frac{\varepsilon^{(2s)}}{\varepsilon^{(1s)}}. \quad (27)$$

This function can be calculated to a rather high accuracy, because it is determined mainly by the behavior of the wavefunctions at the atomic scale and thus almost independent of the nuclear structure [9]. In Table XI we present the numerical results for the parameter  $\xi$  and for the specific difference  $\Delta' E$  between the hyperfine splitting values of H- and Li-like ions. The theoretical accuracy of the presented values  $\Delta' E$  is better than 0.01% and the given uncertainty is determined by the limited knowledge of the nuclear magnetic moments.

Let us summarize: *Ab initio* QED calculations of the ground-state hyperfine splitting of H-, Li-, and B-like ions in the middle- $Z$  region have been performed. The evaluation incorporates results based on a rigorous treatment of first-order many-electron QED effects and on the large-scale CI-DFS calculations of the second- and higher-order electron-correlation effects. The one-loop radiative corrections have been evaluated to all orders in  $\alpha Z$ . The screening QED effect in Li- and B-like sequences have been taken into account utilizing a local Kohn-Sham potential. The Bohr-Weisskopf correction has been calculated employing the single-particle nuclear model. As the result, the most accurate values for the hyperfine splitting of H-, Li-, and B-like ions under consideration have been obtained. The specific difference of the hyperfine splitting values of H- and Li-like ions, where the uncertainties associated with the nuclear-structure corrections are significantly canceled, has been evaluated with an accuracy better than 0.01%.

### Acknowledgments

Stimulating discussions with R. A. Sunyaev are gratefully acknowledged. We also thank A. N. Artemyev for providing us with the computer code for the evaluation of the Wichmann-Kroll electric-loop potential. The authors acknowledge major financial support from DFG, GSI, RFBR

TABLE XI: The parameter  $\xi$  and specific difference  $\Delta'E$  (meV) between the hyperfine structure values of H- and Li-like ions, defined by Eqs. (26) and (25), respectively.

Nucleus	$\mu/\mu_N$	$\xi$	$\Delta'E$
$^{14}\text{N}$	0.40376	0.12531	-0.009955
$^{15}\text{N}$	-0.28319	0.12530	-0.009298
$^{17}\text{O}$	-1.8938(1)	0.12539	-0.04919
$^{19}\text{F}$	2.6289	0.12550	-0.1451
$^{21}\text{Ne}$	-0.66180(1)	0.12561	-0.03029
$^{23}\text{Na}$	2.2175	0.12574	-0.1237
	2.2177	0.12574	-0.1237
$^{25}\text{Mg}$	-0.85545(8)	0.12588	-0.05148
$^{27}\text{Al}$	3.6415	0.12603	-0.2592
$^{29}\text{Si}$	-0.55529(3)	0.12619	-0.07699
$^{31}\text{P}$	1.1316	0.12637	-0.1816
$^{33}\text{S}$	0.64382	0.12656	-0.07904
$^{35}\text{Cl}$	0.82187	0.12676	-0.1151
$^{37}\text{Cl}$	0.68412	0.12676	-0.09587
$^{39}\text{K}$	0.39147	0.12720	-0.07006
	0.39151	0.12720	-0.07007
$^{41}\text{K}$	0.21487	0.12720	-0.03856
	0.21489	0.12720	-0.03857
$^{43}\text{Ca}$	-1.3176	0.12743	-0.2258
$^{45}\text{Sc}$	4.7565	0.12768	-0.9098
$^{47}\text{Ti}$	-0.78848(1)	0.12794	-0.1759
$^{49}\text{Ti}$	-1.1042	0.12794	-0.2347
$^{51}\text{V}$	5.1487	0.12822	-1.213
$^{53}\text{Cr}$	-0.47454(3)	0.12851	-0.1440
$^{55}\text{Mn}$	3.4687	0.12881	-1.044
	3.4532(13)	0.12881	-1.039
$^{57}\text{Fe}$	0.090623	0.12912	-0.04989
	0.090764	0.12912	-0.04996
	0.09044(7)	0.12912	-0.04979(4)
$^{59}\text{Co}$	4.627(9)	0.12945	-1.599(3)
$^{61}\text{Ni}$	-0.75002(4)	0.12979	-0.3307

(Grant No. 07-02-00126a), and INTAS-GSI (Grant No. 06-100012-8881). The work of D.A.G. was also supported by the grant of President of Russian Federation (Grant No. MK-3957.2008.2). N.S.O. acknowledges the support from St. Petersburg Government (Grant No. 75-MU).

---

[1] R. A. Sunyaev and E. M. Churazov, *Pis'ma Astron. Zh.* **10**, 483 (1984) [*Sov. Astron. Lett.* **10**, 201 (1984)].

- [2] R. A. Sunyaev and D. O. Docenko, *Pis'ma Astron. Zh.* **33**, 83 (2007) [*Astron. Lett.* **33**, 67 (2007)].
- [3] I. Klaft, S. Borneis, T. Engel, B. Fricke, R. Grieser, G. Huber, T. Köhl, D. Marx, R. Neumann, S. Schröder, et al., *Phys. Rev. Lett.* **73**, 2425 (1994).
- [4] J. R. Crespo López-Urrutia, P. Beiersdorfer, D. W. Savin, and K. Widmann, *Phys. Rev. Lett.* **77**, 826 (1996).
- [5] J. R. Crespo López-Urrutia, P. Beiersdorfer, K. Widmann, B. B. Birkett, A.-M. Mårtensson-Pendrill, and M. G. H. Gustavsson, *Phys. Rev. A* **57**, 879 (1998).
- [6] P. Seelig, S. Borneis, A. Dax, T. Engel, S. Faber, M. Gerlach, C. Holbrow, G. Huber, T. Köhl, D. Marx, et al., *Phys. Rev. Lett.* **81**, 4824 (1998).
- [7] P. Beiersdorfer, S. B. Utter, K. L. Wong, J. R. Crespo López-Urrutia, J. A. Britten, H. Chen, C. L. Harris, R. S. Thoe, D. B. Thorn, E. Träbert, et al., *Phys. Rev. A* **64**, 032506 (2001).
- [8] D. F. A. Winters, M. Vogel, D. M. Segal, R. C. Thompson, and W. Nörtershäuser, *Can. J. Phys.* **85**, 403 (2007).
- [9] V. M. Shabaev, A. N. Artemyev, V. A. Yerokhin, O. M. Zhrebtsov, and G. Soff, *Phys. Rev. Lett.* **86**, 3959 (2001).
- [10] V. M. Shabaev, *J. Phys. B* **27**, 5825 (1994).
- [11] V. M. Shabaev, M. B. Shabaeva, and I. I. Tupitsyn, *Phys. Rev. A* **52**, 3686 (1995).
- [12] V. M. Shabaev, M. B. Shabaeva, and I. I. Tupitsyn, *Astron. Astrophys. Trans.* **12**, 243 (1997).
- [13] S. Boucard and P. Indelicato, *Eur. Phys. J. D* **8**, 59 (2000).
- [14] K. Pachucki, *Phys. Rev. A* **54**, 1994 (1996).
- [15] M. Nio and T. Kinoshita, *Phys. Rev. D* **55**, 7267 (1997).
- [16] S. G. Karshenboim and V. G. Ivanov, *Eur. Phys. J. D* **19**, 13 (2002).
- [17] P. J. Mohr and B. N. Taylor, *Rev. Mod. Phys.* **77**, 1 (2005).
- [18] S. G. Karshenboim, *Phys. Rep.* **422**, 1 (2005).
- [19] S. A. Blundell, K. T. Cheng, and J. Sapirstein, *Phys. Rev. Lett.* **78**, 4914 (1997).
- [20] P. Sunnergren, H. Persson, S. Salomonson, S. M. Schneider, I. Lindgren, and G. Soff, *Phys. Rev. A* **58**, 1055 (1998).
- [21] V. A. Yerokhin and V. M. Shabaev, *Phys. Rev. A* **64**, 012506 (2001).
- [22] V. A. Yerokhin, A. N. Artemyev, V. M. Shabaev, and G. Plunien, *Phys. Rev. A* **72**, 052510 (2005).
- [23] J. Sapirstein and K. T. Cheng, *Phys. Rev. A* **74**, 042513 (2006).
- [24] P. Pyykkö, E. Pajanne, and M. Inokuti, *Int. J. Quantum Chem.* **7**, 785 (1973).

- [25] A. V. Volotka, V. M. Shabaev, G. Plunien, and G. Soff, *Eur. Phys. J. D* **23**, 51 (2003).
- [26] K. Pachucki, *Phys. Rev. A* **76**, 022508 (2007).
- [27] V. M. Shabaev, M. Tomaselli, T. Kühn, A. N. Artemyev, and V. A. Yerokhin, *Phys. Rev. A* **56**, 252 (1997).
- [28] V. M. Shabaev, M. B. Shabaeva, I. I. Tupitsyn, V. A. Yerokhin, A. N. Artemyev, T. Kühn, M. Tomaselli, and O. M. Zherebtsov, *Phys. Rev. A* **57**, 149 (1998); *ibid* **58**, 1610 (1998).
- [29] O. M. Zherebtsov and V. M. Shabaev, *Can. J. Phys.* **78**, 701 (2000).
- [30] I. I. Tupitsyn, A. V. Loginov, and V. M. Shabaev, *Opt. Spektrosk.* **93**, 389 (2002) [*Opt. Spectrosc.* **93**, 357 (2002)].
- [31] M. Le Bellac, *Nucl. Phys.* **40**, 645 (1963).
- [32] V. M. Shabaev, *Phys. Rep.* **356**, 119 (2002).
- [33] M. B. Shabaeva and V. M. Shabaev, *Phys. Lett. A* **165**, 72 (1992).
- [34] M. B. Shabaeva and V. M. Shabaev, *Phys. Rev. A* **52**, 2811 (1995).
- [35] V. F. Bratzev, G. B. Deyneka, and I. I. Tupitsyn, *Izv. Akad. Nauk SSSR, Ser. Fiz.* **41**, 2655 (1977) [*Bull. Acad. Sci. USSR, Phys. Ser.* **41**, 173 (1977)].
- [36] I. I. Tupitsyn, V. M. Shabaev, J. R. Crespo López-Urrutia, I. Draganić, R. Soria Orts, and J. Ullrich, *Phys. Rev. A* **68**, 022511 (2003).
- [37] D. A. Glazov, V. M. Shabaev, I. I. Tupitsyn, A. V. Volotka, V. A. Yerokhin, G. Plunien, and G. Soff, *Phys. Rev. A* **70**, 062104 (2004).
- [38] V. M. Shabaev, I. I. Tupitsyn, K. Pachucki, G. Plunien, and V. A. Yerokhin, *Phys. Rev. A* **72**, 062105 (2005).
- [39] I. I. Tupitsyn, A. V. Volotka, D. A. Glazov, V. M. Shabaev, G. Plunien, J. R. Crespo López-Urrutia, A. Lapierre, and J. Ullrich, *Phys. Rev. A* **72**, 062503 (2005).
- [40] A. N. Artemyev, V. M. Shabaev, I. I. Tupitsyn, G. Plunien, and V. A. Yerokhin, *Phys. Rev. Lett.* **98**, 173004 (2007).
- [41] W. Kohn and L. J. Sham, *Phys. Rev.* **140**, A1133 (1965).
- [42] D. A. Glazov, A. V. Volotka, V. M. Shabaev, I. I. Tupitsyn, and G. Plunien, *Phys. Lett. A* **357**, 330 (2006).
- [43] N. S. Oreshkina, A. V. Volotka, D. A. Glazov, I. I. Tupitsyn, V. M. Shabaev, and G. Plunien, *Opt. Spektrosk.* **102**, 889 (2007) [*Opt. Spectrosc.* **102**, 815 (2007)].
- [44] Y. S. Kozhedub, D. A. Glazov, A. N. Artemyev, N. S. Oreshkina, V. M. Shabaev, I. I. Tupitsyn, A. V.

- Volotka, and G. Plunien, Phys. Rev. A **76**, 012511 (2007).
- [45] N. S. Oreshkina, D. A. Glazov, A. V. Volotka, V. M. Shabaev, I. I. Tupitsyn, and G. Plunien, Phys. Lett. A **372**, 675 (2008).
- [46] G. Soff and P. J. Mohr, Phys. Rev. A **38**, 5066 (1988).
- [47] N. L. Manakov, A. A. Nekipelov, and A. G. Fainshtein, Zh. Eksp. Teor. Fiz. **95**, 1167 (1989) [Sov. Phys. JETP **68**, 673 (1989)].
- [48] A. G. Fainshtein, N. L. Manakov, and A. A. Nekipelov, J. Phys. B **23**, 559 (1990).
- [49] P. J. Mohr, Ann. Phys. (N.Y.) **88**, 26 (1974); **88**, 52 (1974).
- [50] N. J. Snyderman, Ann. Phys. (N.Y.) **211**, 43 (1991).
- [51] V. A. Yerokhin and V. M. Shabaev, Phys. Rev. A **60**, 800 (1999).
- [52] V. M. Shabaev, I. I. Tupitsyn, V. A. Yerokhin, G. Plunien, and G. Soff, Phys. Rev. Lett. **93**, 130405 (2004).
- [53] I. Angeli, At. Data Nucl. Data Tables **87**, 185 (2004).
- [54] N. J. Stone, At. Data Nucl. Data Tables **90**, 75 (2005).
- [55] M. G. H. Gustavsson and A.-M. Mårtensson-Pendrill, Phys. Rev. A **58**, 3611 (1998).
- [56] V. A. Yerokhin, Phys. Rev. A **78**, 012513 (2008).
- [57] M. Lestinsky, E. Lindroth, D. A. Orlov, E. W. Schmidt, S. Schippers, S. Böhm, C. Brandau, F. Sprenger, A. S. Terekhov, A. Müller, et al., Phys. Rev. Lett. **100**, 033001 (2008).